1-2011

Anti-Amyloid-β Single-Chain Antibody Brain Delivery Via AAV Reduces Amyloid Load But May Increase Cerebral Hemorrhages in an Alzheimer's Disease Mouse Model

Jinghong Kou

Hong-Duck Kim
New York Medical College

Hiroaki Taguchi

Sudhir Paul

Selvarangan Ponnazhagan

See next page for additional authors

Recommended Citation

Kou, J., Kim, H., Pattanayak, A., Song, M., Lim, J. E., Taguchi, H., et al. (2011). Anti-amyloid-beta single-chain antibody brain delivery via AAV reduces amyloid load but may increase cerebral hemorrhages in an Alzheimer's disease mouse model. Journal of Alzheimer's Disease, 27(1), 23-28. doi: 10.3233/JAD-2011-110230

Published in final edited form as:
J Alzheimers Dis. 2011 ; 27(1): 23–38. doi:10.3233/JAD-2011-110230.

Anti-Aβ single-chain antibody brain delivery via AAV reduces amyloid load but may increase cerebral hemorrhages in an Alzheimer mouse model

Jinghong Kou[a], **HongDuck Kim**[b], **Abhinandan Pattanayak**[a], **Min Song**[a,c], **Jeong-Eun Lim**[a], **Hiroaki Taguchi**[d], **Sudhir Paul**[d], **John R. Cirrito**[e], **Selvarangan Ponnazhagan**[f], and **Ken-ichiro Fukuchi**[a,*]

[a]Department of Cancer Biology and Pharmacology, University of Illinois College of Medicine, Peoria, Illinois 61656, USA

[b]Department of Environmental Health Science, New York Medical College, Valhalla, New York 10595, USA

[c]Department of Medical Genetics, Third Military Medical University, Chongqing 400038, PR China

[d]Chemical Immunology Research Center, Department of Pathology and Laboratory Medicine, University of Texas Houston Medical School, Houston, Texas 77030 USA

[e]Department of Neurology and Hope Center for Neurological Disorders, Washington University School of Medicine, St. Louis, Missouri 63110, USA

[f]Department of Pathology, The University of Alabama at Birmingham, Birmingham, Alabama 35294, USA

Abstract

Accumulation of amyloid β-protein (Aβ) in the brain is thought to be a causal event in Alzheimer's disease (AD). Immunotherapy targeting Aβ holds great promise for reducing Aβ in the brain. Here, we evaluated the efficacy and safety of anti-Aβ single-chain antibody (scFv59) delivery via recombinant adeno-associated virus (rAAV) on reducing Aβ deposits in an AD mouse model (TgAPPswe/PS1dE9). First, delivery of scFv59 to the brain was optimized by injecting rAAV serotypes 1, 2, and 5 into the right lateral ventricle. Symmetrical high expression of scFv59 was found throughout the hippocampus and partly in the neocortex in both hemispheres via rAAV1 or rAAV5 while scFv59 expression via rAAV2 was mostly limited to one hemisphere. rAAV1, however, induced apoptosis and microglial activation but rAAV5 did not. Therefore, rAAV5 was selected for therapeutic scFv59 delivery in TgAPPswe/PS1dE9 mice. rAAV5 was similarly injected into the ventricle of 10-month-old TgAPPswe/PS1dE9 mice and 5 months later its efficacy and safety were evaluated. Immunoreactive Aβ deposits reduced in the hippocampus. $Aβ_{42}$ levels in cerebrospinal fluid (CSF) tended to increase and the $Aβ_{40:42}$ ratio decreased in CSF, suggesting that $Aβ_{42}$ was relocated from the parenchyma to CSF. Hemorrhages associated with a focal increase in blood vessel amyloid were found in the brain. While immunotherapy has great potential for clearing cerebral Aβ, caution for cerebrovascular effects should be exercised when rAAV-mediated anti-Aβ immunotherapy is applied.

*Correspondence should be addressed to: Ken-ichiro Fukuchi; kfukuchi@uic.edu. Department of Cancer Biology and Pharmacology, University of Illinois College of Medicine, P.O. Box 1649, Peoria, Illinois 61656, USA; Phone: 309-671-8545, Fax: 309-671-8403.

The authors have no conflicts of interest to disclose.

Keywords

Alzheimer disease; immunotherapy; single-chain antibodies; amyloid; adeno-associated virus; cerebral hemorrhage

INTRODUCTION

Deposition of amyloid β-protein (Aβ) in the brain is one of the pathological hallmarks of Alzheimer's disease (AD) and has been considered to play a critical and possibly causal role in the development of AD [1]. The genetic abnormalities that account for the build-up of Aβ deposits have been identified in some cases of familial AD, such as mutations in the genes encoding Aβ precursor protein (AβPP), presenilin-1 (PS1) and presenilin-2 (PS2), all of which engage in Aβ production. Overexpression of the mutant forms of AβPP in transgenic mice led to AD-like phenotypes including cerebral Aβ deposits and behavioral deficits. Immunization of AD mouse models with synthetic Aβ peptide prevents or reduces Aβ deposits and attenuates memory and learning deficits in animal models of AD [2]. Clinical trials of Aβ vaccination, however, had to be halted because a subset of vaccinated patients (6%) developed brain inflammation presumably induced by T-cell-mediated and/or Fc-mediated immune responses [2–6]. Peripheral administration of anti-Aβ antibodies (passive immunization) also induced clearance of preexisting amyloid plaques in an AD mouse model [7] indicating that an active T-cell-mediated immune response is unnecessary. Thus, passive immunization with anti-Aβ antibody is thought to be a therapeutic option for AD. These earlier studies using AD mouse models suggested Fc receptor-mediated phagocytosis by microglia as the mechanism of Aβ clearance [2,7]. Topical injection of $F(ab')_2$ against Aβ, however, cleared amyloid deposits in an AD mouse model, also [8]. The degree of amyloid clearance by Aβ immunization in an Fc receptor-deficient AD mouse model is similar to that in an Fc receptor-sufficient AD mouse model [9]. These results indicate that amyloid clearance by Aβ immunization does not require Fc-receptor-mediated phagocytosis and that anti-Aβ antibodies without Fc may be a safer treatment due to lack of Fc-mediated immune responses. Reports of human clinical trials indicate that Aβ immunotherapy is effective in clearing Aβ deposits and improving cognitive deficits in a subset of AD patients [3,6,10–12]. Thus, it is important to find a safe, effective immune therapy.

Single chain antibodies (scFvs) lack Fc and are comprised of an antibody heavy chain variable domain linked by a flexible polypeptide linker to a light chain variable domain. By screening the human scFv library, we previously isolated scFvs with high anti-Aβ titers. These scFvs specifically reacted with amyloid plaques and oligomeric Aβ [13]. We previously injected the protein form of a scFv with the highest titer, scFv59, or the scFv59-encoding recombinant adeno-associated virus (rAAV) (Serotype 2) into the corticohippocampal regions of an AD mouse model. In these experiments, expression of scFv was confined to the area in the vicinity of the injection sites, resulting in the limited efficacy in reducing cerebral Aβ deposits [13,14]. In the present study, first we injected three serotypes of rAAV (1, 2 and 5) encoding scFv59 into the right lateral ventricle of mice and then determined levels of scFv59 expression and cytotoxicity in the brain in order to optimize scFv59 brain delivery. Following optimization, we evaluated therapeutic effects of scFv59 delivery on Aβ clearance and safety in an AD mouse model using optimized rAAV.

MATERIAL AND METHODS

Recombinant adeno-associated virus preparation

Expression of plasmid vectors, pAAV-CAscFv59 and pAAV-CAscFv-Gag, for rAAV production were described previously [14]. Briefly, pAAV-CAscFv was constructed by

cloning scFv cDNA under the control of cytomegalovirus enhancer/β-actin promoter in a rAAV expression plasmid. In the vectors, the Kozak sequence and woodchuck hepatitis virus post-transcriptional regulatory element were included to increase the transcription and translation efficiency, respectively. FLAG-His tag was placed at the C-terminal ends of scFv as a marker. pAAV-CAscFv59 encodes scFv59 that reacts with oligomeric Aβ as well as Aβ deposits in the brain [13]. pAAV-CAscFv-Gag encodes scFv-Gag that binds to HIV Gag [14]. Using the calcium phosphate transfection method as previously described [15], HEK293 cells were transfected with pAAV-CAscFv59 and one of the following helper plasmids, pDP1, pDG, and pDP5, to produce pseudotyped rAAV1, rAAV2 and rAAV5 encoding scFv59, respectively. The helper plasmids carried both the AAV2 *rep2* gene and one of the serotype specific *cap* genes [15]. Produced viral particles were released from the cells by rapid freeze and thaw and purified by iodixanol gradient centrifugation. The iodixanol gradient fraction was further purified by HPLC using a 5-ml HiTrap Q column (GE Healthcare, Piscataway, NJ) as described before [16]. A control rAAV5 encoding scFv-Gag was similarly prepared. The titers of rAAV virions that contained the vector genomes were determined by the quantitative dot-blot assay as described previously [14].

Experimental animals and stereotaxic injection of rAAV-scFvs

C57BL/6 mice (6–8 weeks old) purchased from Jackson Laboratory (Bar Harbor, ME) were used to optimize intracranial delivery of scFv59 by testing 3 differently pseudotyped rAAVs. Mice were randomly assigned to 4 treatment groups in such a manner as there was no significant intergroup difference in body weight: PBS, rAAV1-CAscFv59, rAAV2-CAscFv59 and rAAV5-CAscFv59 group (n = 10 for each group). Mice were anesthetized by pentobarbital and placed on a stereotaxic instrument with a motorized stereotaxic injector (Stoelting, Wood Dale, IL). A midline incision was made to expose the bregma. A hole in the skull was made by a drill 0.5 mm posterior to the bregma and 1.0 mm right to the midline. rAAV [2.5×10^{10} vector genomes (vg) in 10 μl PBS/mouse] was injected unilaterally into the right ventricle at the depth of 2 mm at a rate of 1 μl/min. After allowing the needle to remain in place for 5 min, the needle was slowly raised at a rate of 0.1 cm/min. Control mice received the same amount of PBS. Three months after the rAAV injection, the experimental mice were terminated by a lethal injection of sodium pentobarbital to determine expression levels of scFv59 in the brain. An AD mouse model, B6.Cg-Tg(APPswe, PSEN1dE9) 85Dbo/J mice (TgAPPswe/PS1dE9 mice) [17] purchased from Jackson Laboratory, was used to study the therapeutic effects of intracerebroventricular injection of the optimized rAAV-CAscFv59. Ten-month-old TgAPPswe/PS1dE9 mice (n = 10, 8 mice for histochemical analyses and 2 mice for western blot analysis of scFv59 expression) were subjected to a single injection of rAAV5-CAscFv59 (3.0×10^{10} vg/mouse) into the right lateral ventricle as described above. As controls, age- and sex-matched TgAPPswe/PS1dE9 mice received the same amount of rAAV5-CAscFv-Gag (n = 8) or PBS (n = 10). Five months after the rAAV injection, the experimental animals were terminated to determine the therapeutic effects of the treatment. All animal protocols used for this study were prospectively reviewed and approved by the Institutional Animal Care and Use Committee of the University of Illinois College of Medicine at Peoria.

Murine CSF isolation

Cerebrospinal fluid (CSF) was isolated from the cisterna magna compartment using the method described by DeMattos et al. [18]. Mice were anesthetized by pentobarbital and fixed facedown on a narrow platform. An incision was made from the top of the skull to the dorsal thorax. The musculature from the base of the skull to the first vertebrae was carefully removed to expose the meninges overlying the cisterna magna. The surrounding area was gently cleaned with 1x PBS using cotton swabs to remove any residual blood or other interstitial fluid. The arachnoid membrane covering the cistern was punctured with a 29

gauge insulin syringe. A polypropylene narrow bore pipette was immediately placed in the hole to collect CSF. As the primary CSF exiting the compartment was collected, a second collection was performed after the cistern was refilled within 2 min. About 10 to 15 μl CSF was collected from each mouse.

Quantification of CSF Aβ by ELISA

Aβ levels in CSF were quantified by the $A\beta_{42}$ and $A\beta_{40}$ enzyme-linked immunosorbent assay (ELISA) kits (Invitrogen, Carlsbad, CA) according to the manufacturer's protocol.

Immunohistochemical and histochemical analyses

Mice were deeply anesthetized with pentobarbital and cardinally perfused with cold PBS followed by 4% paraformaldehyde. The brains were quickly removed and fixed in 4% paraformaldehyde for 16 h. The brains were then stored overnight in 30% sucrose in 0.1M PBS and frozen in Tissue-Teck optimal cutting temperature compound. For C57BL/6 mice, frozen sections (5 μm thick) were prepared and subjected to immunohistochemical and TUNEL staining. The brain sections were immunostained with anti-FLAG M2 monoclonal antibody (scFv contains Flag sequences as a marker) (Sigma, St. Louis, MO) for detection of scFv59. Neuroinflammation was detected by staining the brain sections with rat anti-mouse CD11b, rat anti-mouse CD45, rabbit anti-mouse GFAP antibodies (Serotec, Oxford, UK) and rabbit anti-ionized calcium binding adaptor molecule 1 (Iba1) antibody (Wako, Richmond, VA). The avidin-biotin immunoperoxidase method was carried out for immunohistochemistry using Vectastain ABC kit (Vector, Burlingame, CA) and 3,3′-diaminobenzidine as previously described [19]. For the negative control, slides were processed without primary antibody. For TgAPPswe/PS1dE9 mice, coronal sections (35 μm thick) of the brains were cut on a freezing-stage cryotome and kept in 0.1 M PBS at 4°C. Sections were subjected to immunohistochemical, histochemical, and TUNEL staining. For immunohistochemistry, free floating immunohistochemistry was performed using avidin-biotin immunoperoxidase method (Vector). Endogenous peroxidase was eliminated by treatment with 1% H_2O_2/10% methanol Tris-buffered saline (TBS) for 60 min at room temperature. After washing with 0.1 M Tris buffer (pH 7.5) and 0.1 M TBS (pH 7.4), sections were blocked with 5% normal serum (from the same animal species in which the secondary antibody was made) in 0.1M TBS with 0.5% triton-X-100 (TBS-T) for 60 min at room temperature to prevent non-specific protein binding. The sections were then incubated with primary antibodies as described above in TBS-T for 18–48 h at 4°C. For detection of Aβ, $A\beta_{40}$ and $A\beta_{42}$, sections were similarly incubated with 6E10, $A\beta_{40}$- and $_{42}$- specific monoclonal antibodies, respectively (Signet). The sections were rinsed in 0.1 M TBS and incubated with biotinylated secondary antibodies in 2% serum TBS-T for 2 h at room temperature. Finally, the avidin biotin peroxidase method using 3,3′-diaminobenzidine as a substrate (Vector) was performed. This staining protocol was optimized for detection of amyloid plaques without labeling intracellular AβPP. For the negative control, slides were processed without primary antibody. Some sections were counterstained with hematoxylin.

For detection of possible cerebral hemorrhages that may be associated with scFv treatment, Prussian blue reaction was carried out on brain sections using an Iron Stain kit (Sigma-Aldrich, St. Louis, MO) according to the manufacturer's protocol.

Histomorphometry for quantification of amyloid deposits and reactive/activated glial cells was performed using an Olympus BX61 automated microscope, Olympus Fluoview system and the Image Pro Plus v4 image analysis software (Media Cybernetics, Silver Spring, MD) capable of color segmentation and automation via programmable macros. Five to seven coronal brain sections, each separated by an approximately 400 μm interval, starting at 1.3 mm posterior to the bregma to caudal, from each mouse were analyzed. Both neocortex and

hippocampus were found in all the brain sections and analyzed separately. Stained areas were expressed as a percentage of total neocortex or hippocampus, respectively. Quantitative analysis of vascular amyloid was performed on 6E10-stained sections. The total pixels of Aβ-positive vessels were counted and calculated as per mm^2 of the hippocampal area. Data were expressed as mean ± standard error of the mean (SEM) as a bar graph.

TUNEL assay to detect apoptosis

To investigate cytotoxicity possibly associated with the therapeutic modalities, brain sections were subjected to Terminal (TdT)-mediated dUTP-biotin nick end labeling (TUNEL) assay using the *In situ* Cell Death Detection Kit (Roche Biochemicals, Indianapolis, IN) according to the manufacturer's protocol. Slides were analyzed using an Olympus BX61 automated microscope, Olympus Fluoview system.

Immunoblotting for detection of scFv in the CSF and brain

Hippocampal and neocortex homogenates (50 μg) or CSF samples (10 μl) were mixed with 5 x sample buffer (final concentration: 60mM Tris-HCl, 2% SDS, 10% glycerol, 0.001% bromphenol blue, pH: 6.8) and heated at 100°C for 5 min. Samples were subjected to 10–20% Tris-HCl gradient SDS-PAGE and electrotransferred to polyvinylidine difluoride (PVDF) membranes (Millipore, Bedford, MA). scFvs on the membranes were detected using anti-flag biotinylated M2 monoclonal antibody (Sigma) and then visualized by an enhanced chemiluminescence system (Amersham, Arlington Heights, IL) according to the manufacturers' protocol.

Determination of anti-scFv antibody titers in sera

Two and five months after the intracerebroventricular injection of rAAVs, blood samples were collected to determine levels of anti-scFv antibodies which were possibly raised in mice subjected to rAAV5-CAscFv59 injection. Briefly, approximately 100 μl of blood per mouse was taken from the tail vein and incubated at room temperature for 1 h then transferred to 4°C. After overnight incubation, blood was centrifuged at 12,000 × g for 30 min and serum was stored at −80°C and thawed at the time of assay. ELISA was carried out to determine titers of anti-scFv antibodies. Briefly, 96-well plates were coated with 500 ng purified scFv59 per well at 4°C overnight, followed by incubation with blocking buffer (1x PBS containing 0.5% BSA, 0.05% Tween-20 and 5% goat serum) at room temperature for 1 h. Then, diluted serum samples (1:50) were added to microtiter wells and incubated at 4°C overnight. The next day, the microplates were washed 5 times using washing buffer (1x PBS containing 0.05% Tween-20), and then incubated with HRP-conjugated secondary antibody at room temperature for 1 h. The microplates were then washed with washing buffer 5 times followed by incubation with 3,3′,5,5′-tetramethylbenzidine (TMB) (Kirkegaard & Perry Laboratories Inc., Gaithersburg, MD) for 15 min to allow the development of the color. The reaction was stopped by adding 100 μl of 1 N H_2SO_4. The optic densities were determined at 450 nm using a Microplate Reader. Serial dilutions of anti-FLAG M2 antibody were used as standard to determine titers of anti-scFv antibodies.

Statistical analysis

Data were expressed as mean ± SEM. Analysis of variance (ANOVA) and two-tailed Student's t-test were used to determine the intergroup significant difference, except for hemorrhage frequencies where chi-square analysis was used. $P < 0.05$ was considered statistically significant.

RESULTS

Transduction efficiency of rAAV serotype 1, 2, and 5 in the brain by intraventricular injection in *adult C57BL/6 mice*

Three serotypes of rAAV (1, 2 and 5) encoding scFv59 were tested in adult C57BL/6 mice to determine the optimal rAAV serotype for intracranial delivery of anti-Aβ scFv. The rAAV-CAscFv59 vectors [2.5×10^{10} vector genomes (vg)/ventricle] were injected into the right ventricle with the purpose of distributing rAAV to broader areas in the brain by CSF flow for widespread transduction. In the rAAV-CAscFv59 vectors, cDNA for scFv59 was placed under the control of cytomegalovirus enhancer/β-actin promoter [14]. Three months after injection, the mice were euthanized to evaluate the transduction efficiency of each rAAV serotype. The brain sections were subjected to immunohistochemistry using anti-FLAG M2 antibody to visualize expressed scFv59 (scFv59 contains the Flag sequence as a marker).

In the brains of rAAV1- and rAAV5- injected mice, widespread high expression of scFv59 was observed throughout the hippocampi and partly in the neocortexes along the ventricles and hippocampi in both hemispheres in 9 out of 10 experimental mice for both groups (Figure 1b, d). Not only cell bodies but also the neuropil of hippocampi and neocortexes were heavily stained with anti-FLAG M2 antibody, suggesting secretion of scFv59 from cells. Even though rAAV1 and rAAV5 were injected into only the right ventricle, their staining patterns appeared to be symmetrical (Figure 1b, d), suggesting a systemic spread of rAAV through CSF flow and/or neuronal pathways in the brain.

In the brains of rAAV2-injected mice, expression of scFv59 was limited mostly to a small part of the hippocampus (Figure 1c). Only 4 out of 10 mice subjected to AAV2 injection showed such positive staining, including 2 mice in which scFv59 expression was found in both hemispheres.

rAAV1-mediated scFv 59 brain delivery causes microglial activation and apoptosis in C57BL/6 *mice*

High levels of neural scFv expression may be cytotoxic and activate glial cells. For example, overexpressed scFv may cross-react with intracellular essential components in certain signaling pathways or specifically deplete the antigen, leading to altered cell metabolism, apoptosis and/or inflammatory responses. To assess cytotoxicity and inflammation potentially associated with AAV-mediated brain expression of scFv59, brain sections were subjected to TUNEL assay and immunohistochemistry, respectively, using anti-GFAP antibody for reactive astrocytes and anti-CD11b, CD11c and CD45 antibody for activated microglia/monocytes.

No cell death was detected by TUNEL in the brains subjected to rAAV2, rAAV5 and PBS injection (Figure 1e, g, h). In contrast, TUNEL-positive cells were scattered in the hippocampi of mice subjected to rAAV1 injection (Figure 1f), indicating that rAAV1-mediated scFv59 expression is harmful to hippocampal cells. In line with these observations, CD11b-immunoreactive cells were found in the hippocampi of rAAV1-injected mice (Figure 1j) but not in PBS-, rAAV2- and rAAV5-injected mice (Figure 1i, k, l), suggesting inflammation in response to apoptotic cells. No difference, however, was found in CD11c, CD45 and GFAP immunoreactivity in the brain between any groups including PBS-injected mice (data not shown).

Thus, extensive, high expression of scFv59 was achieved throughout the hippocampus and partly in the neocortex by unilateral intraventricular injection of rAAV1 and rAAV5. Because rAAV1-mediated expression of scFv59 was associated with apoptosis and activated

microglia, rAAV5 was selected for testing the therapeutic efficacy of scFv59 in an AD mouse model.

High scFv59 expression via rAAV5 in the hippocampus inTgAPPswe/PS1dE9 mice

TgAPPswe/PS1dE9 mice (an AD mouse model) start to develop Aβ deposits in the brain between 4 and 5 months of age and have numerous amyloid plaques at 10 months of age. Therefore, rAAV5 encoding scFv59 (3×10^{10} vg/mouse), rAAV5-CAscFv59, was injected into the right lateral ventricle of 10-month-old TgAPPswe/PS1dE9 mice to evaluate the therapeutic efficacy of rAAV5-mediated scFv59 expression in the brain. As controls, age- and sex-matched TgAPPswe/PS1dE9 mice were similarly injected with PBS or rAAV5 encoding scFv-Gag, rAAV5-CAscFv-Gag. scFv-Gag specifically immunoreacts with HIV-1 Gag [14].

Five months after injection, expression levels of scFv59 in the brain and CSF were determined by immunohistochemistry and western blotting, respectively, using anti-FLAG M2 antibody. By immunohistochemistry, widespread high expression of scFv59 or scFv-Gag was observed in the hippocampi in both hemispheres in rAAV5-injected mice (Figure 2b, c). Strong immunoreactivity for scFv was found in both neuronal cell bodies (Figure 2d) and the neuropil (Figure 2e) in the hippocampus, suggesting intracellular accumulation of scFv as well as scFv secretion from the cells, respectively. The staining of the neocortex however, was less intense than that of the hippocampus (Figure 2b, c). By western blotting, scFv59 was identified as an approximately 30 kDa fragment in the CSF from TgAPPswe/PS1dE9 mice subjected to rAAV5-CAscFv59 injection (Figure 2f). By comparison with the intensity of purified scFv59 (10 ng) on the western blot, levels of scFv59 expression in the CSF were estimated to be approximately 1 ng/μl (~30 nM). In the hippocampus, scFv59 was identified as 30–35 kDa fragments (Figure 2g) and estimated to be 1–2 ng/μg protein by the same method. In the neocortex, however, scFv59 was undetectable by western blotting.

rAAV5-mediated scFv59 brain delivery reduces Aβ load in the hippocampus in TgAPPswe/PS1dE9 mice

To determine the efficacy of rAAV5-mediated scFv59 expression in reducing Aβ load in the brain, Aβ deposits were detected by immunohistochemistry using anti-Aβ 6E10 antibody and quantified by morphometry (Figure 3a–d). The amyloid load was expressed as the percentage of area showing Aβ immunoreactivity. The average Aβ loads in hippocampus were 0.39 ± 0.09, 0.65 ± 0.15 and 0.70 ± 0.06% for mice subjected to rAAV5-CAscFv59, rAAV5-CAscFv-Gag and PBS injection, respectively (Figure 3d). Thus, rAAV5-CAscFv59 injection reduced the Aβ load in the hippocampus by approximately 45% as compared with PBS injection ($P = 0.01$, n = 8 for each group). In the neocortex, the average amyloid load in rAAV-CAscFv59-injected mice (1.14 ± 0.15%) was less than those in rAAV-CAscFv-Gag-injected (1.32 ± 0.18%) and PBS-injected (1.30 ± 0.15%) mice but the difference was not significant (scFv59 vs. PBS, $P = 0.1$).

Because rAAV-CAscFv59 injection reduced the average Aβ load in the hippocampus but not in the neocortex by 6E10 immunoreactivity, we further investigated hippocampal Aβ loads by $Aβ_{40}$ and $Aβ_{42}$ C-terminal-specific antibodies. rAAV-CAscFv59 injection also reduced the average $Aβ_{42}$ load in the hippocampus (0.20 ± 0.028% for rAAV-CAscFv59 and 0.30 ± 0.034% for PBS, $P < 0.05$) (Figure 3e–g). rAAV-CAscFv59 injection tended to reduce $Aβ_{40}$ loads in the hippocampus (0.18 ± 0.025%) compared to PBS injection (0.23 ± 0.034%) but the difference was not significant.

Lack of reactive gliosis associated with rAAV5-mediated scFv59 expression in the hippocampus *in TgAPPswe/PS1dE9 mice*

The Aβ load in the hippocampus reduced in rAAV5-CAscFv59-injected mice compared with PBS-injected mice but did not reduce it in the neocortex. We determined if the decrease in the Aβ load in the hippocampus was associated with alterations in glial activation using immunohistochemistry. Reactive astrocytes were immunostained with anti-GFAP antibody and activated microglia and infiltrating leukocytes were detected by anti-CD11b and CD45 antibody, respectively. Representative micrographs of the hippocampus from TgAPPswe/PS1dE9 mice subjected to rAAV5- and PBS-injection are shown in Supplementary Figure 1a–c for CD11b, Supplementary Figure 2a–c for CD45 and Supplementary Figure 3a–c for GFAP. Gliosis was expressed as the percentage of area showing immunoreactivity (Supplementary Figure 1d for CD11b, Supplementary Figure 2d for CD45 and Supplementary Figure 3d for GFAP). Morphometric analysis of the immunostaining revealed no differences in immunoreactivity for GFAP, CD11b, and CD45 between any groups.

rAAV5-mediated scFv59 brain delivery alters the $A\beta_{40}$:$A\beta_{42}$ ratio in CSF in TgAPPswe/PS1dE9 *mice*

scFv59 was found in the CSF of rAAV5-CAscFv59-injected mice and may affect Aβ metabolism in the CSF. Therefore, levels of Aβ in CSF were determined by the Aβ40- and Aβ42-specific ELISAs (Figure 4). $A\beta_{40}$ levels in rAAV5-CAscFv59-injected mice (1.99 ± 0.41 ng/ml, n = 8) were similar to those in rAAV5-CAscFv-Gag-injected (2.03 ± 0.58 ng/ml, n = 8) and PBS-injected (2.39 ± 0.51 ng/ml, n = 8) mice. CSF $A\beta_{42}$ levels in rAAV5-CAscFv59-injected mice (0.55 ± 0.1 ng/ml) are approximately 40% higher than those in PBS-injected mice (0.39 ± 0.06 ng/ml) but this did not reach statistical significance (P = 0.1). $A\beta_{42}$ levels in rAAV5-CAscFv-Gag-injected mice (0.28 ± 0.08 ng/ml) were also lower than those in rAAV5-CAscFv59-injected mice (P = 0.04) but not different from those in PBS-injected mice. The $A\beta_{40:42}$ ratio in CSF was significantly lower in rAAV5-CAscFv59-injected mice (3.94 ± 0.6) than that in rAAV5-CAscFv-Gag-injected (7.14 ± 1.11, P = 0.02) and PBS-injected (6.37 ± 0.97, P < 0.05) mice (Figure 4).

rAAV5-mediated scFv59 brain delivery may cause cerebral hemorrhages

To study cytotoxicity possibly associated with expression of scFv59 via rAAV5, brain sections from TgAPPswe/PS1dE9 mice subjected to rAAV5-CAscFv59-, rAAV5-CAscFv-Gag- and PBS-injection were evaluated by TUNEL assay 5 months after the injection. For each mouse (n = 8 for each group), 5 coronal brain sections separated by consecutive ~400 μm, starting at the injection site (0.5 mm posterior to the bregma) toward the caudal direction were analyzed. No difference was seen among the treatment groups in TUNEL labeling (data not shown), suggesting that therapeutic expression of scFv59 is not toxic to cells.

Because anti-Aβ immunotherapy was reported to cause cerebral microhemorrhages in AD mouse models and a patient with AD, possible cerebral hemorrhage was investigated by iron staining. Brain sections from the 3 mouse groups were analyzed as described in the TUNEL assay above except that 7 coronal brain sections from each mouse were analyzed. Scattered stains along with the needle tracks at the injection sites were found in several mice in all experimental groups even 5 months after the injection (Figure 5a). Hemorrhages associated with blood vessels were rare but clearly detected in 2 mice subjected to rAAV5-CAscFv59-injection: one in the hippocampus and another along the corpus callosum (Figure 5b). Proximal to the hemorrhage sites, strong, circumferential Aβ immunoreactivity was found in blood vessels (Figure 5c, d). Hemorrhages and circumferential Aβ-positive blood vessels in the hippocampus and corpus callosum were not found in PBS- and rAAV5-CAscFv-Gag-

injected mice. Hemorrhages associated with Aβ immunotherapy are often accompanied by an increase in cerebral amyloid angiopathy (CAA) [10,20–22]. Aβ-immunoreactive blood vessels were quantified by morphometry. On average, rAAV5-CAscFv59-injected mice (165 ± 76 pixels/mm^2) had a two-fold increase in average signal intensity of hippocampal Aβ-immunoreactive blood vessels compared with PBS-injected mice (82 ± 55 pixels/mm^2) but the difference was not significant due to large individual variation (Figure 5e). The statistical significance of the hemorrhages in mice treated with rAAV5-CAscFv59 (n = 8) was compared with the other groups (n = 16) using the chi-squared test. This trend of hemorrhage in rAAV5-CAscFv59-injected mice did not reach statistical significance (P = 0.06). Thus, expression of scFv59 in the brain may cause isolated cerebral hemorrhages and an increase in Aβ deposits in the focal blood vessels.

Lymphocytic and macrophage infiltration was not observed in the brains of any mouse groups, indicating that rAAV-mediated scFv59/scFv-Gag delivery did not cause meningoencephalitis. Small areas of mild gliosis were found along the needle tracks in all groups including PBS-injected mice.

Anti-scFv59 antibodies induced by rAAV5-mediated scFv59 expression in the brain are negligible

scFv59 was derived from a human antibody phage library and may induce immune responses in mice leading to inactivation of scFv59. To determine whether intracerebroventricular injection of rAAV5-CAscFv59 results in anti-scFv59 antibody production, blood was obtained from TgAPPswe/PS1dE9 mice subjected to rAAV5-CAscFv59-injection and the titers were quantified by ELISA. Out of 8 mice, 4 mice had anti-scFv59 titers in their blood ranging from 3 to 91 ng/ml 5 months after the injection (Figure 6). Thus, anti-scFv59 antibodies were discernible in some mice after rAAV5-CAscFv59 treatment. Their titers, however, were very modest and appeared to have insignificant effects on inactivating scFv59, which was estimated to be approximately 1 μg/ml in the CSF.

DISCUSSION

It is possible to achieve widespread neuronal transduction and long-term expression of a transgene in the brains of rodents by injecting rAAV1 vectors into the lateral ventricles of neonatal mice [23–25]. Unilateral injection of rAAV1 and rAAV5 into the striatum on neonatal rats induced unilaterally widespread brain transduction and rAAV5 produced more widespread transgene expression than rAAV1, particularly in the hippocampus and septum [26]. The efficacy of transduction is largely influenced by titers of viral vectors and promoters that drive transgenes. However, it is difficult to obtain widespread neuronal transduction in adult rodents, which is essential to testing the therapeutic efficacies of gene delivery in adult rodent models of certain diseases, including AD. When striatum injection of rAAV serotype 1–6 vectors was tested in the primate brain, AAV5 was the most efficient vector, capable of transducing significantly more cells than any other serotypes [27]. In line with this observation, rAAV5 has been shown to be more efficient than rAAV1 in brain transduction in adult mice when injected into the striatum [28].

A comparative evaluation of brain transduction efficacy by unilateral ventricular injection of these AAV serotypes has not been conducted. Therefore, we have tested for brain transduction efficacies of these vectors by delivering rAAV serotype 1, 2 and 5 into the right lateral ventricle of adult mice. Our results demonstrate that strong expression of scFv59 was achieved equally among rAAV1 and rAAV5 injection throughout the hippocampus and partly in the frontal and parietal cortex next to the hippocampus. We also show that the expression pattern of scFv59 was symmetrical in both hemispheres although they were

unilaterally injected. The symmetrical expression pattern may be due to distribution of rAAV vectors to broader areas in the brain by CSF flow. Alternatively, transportation of rAAV along neuronal pathways in the corpus callosum may lead to the symmetrical expression pattern.

Expression of scFv in animals may induce production of antibodies against scFv resulting in neutralization of scFv. rAAV5-mediated scFv59 delivery to the brain elicited very modest antibody titers (less than 0.7 nM) against scFv59 in a minor subset of mice. Because 1% or less antibodies in the circulation can cross BBB [7,29] and because the estimated concentration of scFv59 in CSF is 30 nM, the neutralizing activity of the induced antibodies against scFv59 is negligible.

Previous studies have shown that intracranial delivery of anti-Aβ scFvs via rAAV1 or rAAV2 was effective in reducing cerebral Aβ load and/or improving learning deficits in AD mouse models [14,30–33]. No adverse effect was noted in these studies. In contrast, scFv59 delivery to the brain by rAAV1 in the present study induced scattered apoptosis and microglial activation mostly in the hippocampus. The patterns and degree of scFv59 expression in the brain via rAAV1 and rAAV5 were similar, but rAAV5-mediated expression did not induce such adverse effects. The molecular mechanism of the adverse effects remains to be elucidated. Because expression of green fluorescent protein, a widely used, nontoxic marker protein, via rAAV1 and rAAV5 is associated with cytotoxicity in cultured neural cells at high doses [34,35] and because differences in cell tropism between rAAV1 and rAAV5 have been reported [26,27,34–37], it is possible that certain types of cells that are selectively transduced by rAAV1 are vulnerable to a high concentration of scFv59. Alternatively, since rAAV1 reaches peak expression faster than rAAV5 (for example, within 4 days vs. 14 days, respectively) [37,38], certain cell types may be unable to adapt to rapid changes in protein synthesis, resulting in apoptosis and microglial activation.

rAAV5-mediated scFv59 delivery significantly reduced $A\beta_{42}$ load in the hippocampus but a decrease in $A\beta_{40}$ load was not significant (Figure 3e–g). A preferential reduction of insoluble $A\beta_{42}$ has been reported when scFv against Aβ (Aβ-scFv) was delivered to the hippocampus of an AD mouse model via rAAV1, also [33]. The reasons for the preferential reduction in $A\beta_{42}$ are not clear. Both scFv59 and Aβ-scFv were isolated by screening human scFv phage libraries for $A\beta_{42}$ immunoreactivity, appeared to recognize conformational epitopes instead of linear epitopes of $A\beta_{42}$, and inhibited $A\beta_{42}$-mediated cytotoxicity[13,33]. Therefore, their characteristics in common may be responsible for the preferential reduction in $A\beta_{42}$. Another possible reason is that the difference in $A\beta_{42}$ load is more discernible than that in $A\beta_{40}$ load because the amounts of insoluble $A\beta_{42}$ deposits are much larger than those of insoluble $A\beta_{40}$ deposits in the brains of these AD mouse models [33,39].

Human clinical trials of Aβ immunization (AN1792) and passive immunization induced microhemorrhages and vasogenic edema in the cerebral blood vessels in an AD patient and some AD mouse models. Such hemorrhages were associated with an increase in blood vessel Aβ deposits (cerebral amyloid angiopathy, CAA) [10,20–22]. CAA is recognized as a cause of brain hemorrhage, and Aβ deposits in CAA are thought to induce degeneration of smooth muscles and weaken blood vessel integrity [40]. We found cerebral hemorrhages in 15-month-old TgAPPswe/PS1dE9 mice subjected to rAAV5-CAscFv59 injection, which were closely associated with strong, circumferential Aβ-positive blood vessels. Neither hemorrhages nor circumferential Aβ-positive blood vessels were found in the other 2 groups. Thus, our mouse models of AD may be useful to recapitulate the side effects of anti-Aβ immunotherapy. No hemorrhage was reported in previous studies where anti-Aβ scFv

was delivered into the brain via rAAV [14,24,31–33]. The discrepancy may be due to (1) prophylactic application of anti-Aβ scFv prior to buildup of Aβ plaques, thereby eliminating relocation of parenchymal Aβ deposits to the blood vessels, (2) the younger age of mice used in the previous studies, at which hemorrhages are too infrequent, (3) use of rAAV2, which may enable only limited scFv accumulation or only region-specific scFv accumulation, thereby precluding damage to the vessels, and/or (4) differences in scFv molecular characteristics, including differences in epitopes recognized by the different scFv constructs and their ability to form potentially harmful multimers. One of the mechanisms explaining the increased hemorrhage after anti-Aβ immunotherapy is that Aβ in parenchymal amyloid plaques is solubilized by anti-Aβ antibody and focally relocated to the blood vessels [41,42]. In support of this view, Aβ deposits in CAA increased only in the specific brain area where the highest extent of parenchymal amyloid plaque clearance was observed [41,43]. We also did not observe a global increase in Aβ deposition in the blood vessels, further supporting this mechanism. Furthermore, Nicoll et al. [44] recently demonstrated that formation of IgG immune complexes in the blood vessel walls enhanced the accumulation of substances solubilized from the extracellular space and proposed this process as the mechanism of the increased CAA after Aβ immunotherapy. Although scFv constructs are devoid of the Fc region found in IgG, scFv-Aβ immune complexes may increase accumulation of solubilized Aβ in the blood vessels by a similar mechanism. Moreover, certain scFv constructs can form large, noncovalent multimers by unintended intermolecular pairing of the variable domains [45], and immune complexes containing the large multimers can be conceived to be detrimental to the physical integrity of the vessels. One of mechanisms proposed for hemorrhages associated with CAA is inflammatory responses including reactive astrocytes and activated microglia. We, however, did not find increases in reactive astrocytes immunoreactive to GFAP and activated microglia/macrophages immunoreactive to CD11b, CD45, and Iba1 (data not shown) in the vicinity of blood vessels in the hippocampi of rAAV5-CAscFv59-injected mice compared with PBS-injected mice. Our results are consistent with the concept that Fc-mediated activation of microglia/macrophages is not the sole event in Aβ immunotherapy leading to hemorrhage [46].

Transgenic mice carrying a mutant form of AβPP found in hereditary cerebral hemorrhage with amyloidosis-Dutch type have a high $A\beta_{40:42}$ ratio in brain parenchymal tissue and develop extensive CAA with few parenchymal amyloid plaques [47]. The ε4 allele of apolipoprotein E (apoE) is a risk factor for CAA as well as AD. Interestingly, Tg2576 mice carrying a targeted replacement of the apoE gene with the human apoE4 allele develop substantial CAA with very few parenchymal amyloid plaques and have an elevated ratio of $A\beta_{40:42}$ in brain extracellular pools and a lower $A\beta_{40:42}$ ratio in CSF [48]. Thus, a higher $A\beta_{40:42}$ ratio in the brain parenchyma has been hypothesized to favor the formation of CAA over parenchymal plaque pathology. Although we did not quantify the $A\beta_{40:42}$ ratio in the brain parenchyma, the mouse group subjected to rAAV5-CAscFv59 injection had a lower $A\beta_{40:42}$ ratio in CSF compared to the other two groups. Thus, anti-Aβ antibodies that increase the $A\beta_{40:42}$ ratio in the parenchymal tissue and decrease it in CSF may exacerbate CAA and cerebral hemorrhage.

Mouse models of AD have been criticized recently because of their failure to predict side effects found in the clinical trials. Our results suggest that rAAV-mediated delivery of genetically modified antibodies against Aβ to various tissues and cells in AD models can be useful for systematic evaluation of the mechanisms underlying Aβ clearance by anti-Aβ immunotherapy and its side effects such as hemorrhage and inflammation. The finding of cerebral hemorrhages associated with rAAV-mediated anti-Aβ antibody delivery raises concerns because the vast majority of AD patients have CAA, and hemorrhages associated with CAA can be detrimental to AD patients [40]. Our studies indicate that rAAV5-

mediated therapeutic delivery of anti-Aβ scFv reduced Aβ load in the hippocampus but was associated with a lower $A\beta_{40:42}$ ratio in CSF, a focal increase in blood vessel Aβ deposits, and cerebral hemorrhages. Thus, while Aβ immunotherapy remains promising, caution should be exercised when rAAV-mediated anti-Aβ immunotherapy is applied. Finding new strategies to minimize the side effects of immunotherapy is advisable. Recently, catalytic antibodies that permanently degrade Aβ without forming stable immune complexes have been described [49]. Such catalysts hold the potential of Aβ immunotherapy while minimizing the risk of hemorrhages.

Supplementary Material

Refer to Web version on PubMed Central for supplementary material.

Acknowledgments

This work was supported in part by grants from the National Institutes of Health (EY018478, AG029818, AG037814, and AG030399) and Alzheimer's Association (IIRG-07-59494). We thank Linda Walter for assistance in preparation of this manuscript.

References

1. Hardy J, Selkoe DJ. The amyloid hypothesis of Alzheimer's disease: progress and problems on the road to therapeutics. Science. 2002; 297:353–356. [PubMed: 12130773]
2. Schenk D, Barbour R, Dunn W, Gordon G, Grajeda H, Guido T, Hu K, Huang J, Johnson-Wood K, Khan K, Kholodenko D, Lee M, Liao Z, Lieberburg I, Motter R, Mutter L, Soriano F, Shopp G, Vasquez N, Vandevert C, Walker S, Wogulis M, Yednock T, Games D, Seubert P. Immunization with amyloid-beta attenuates Alzheimer-disease-like pathology in the PDAPP mouse. Nature. 1999; 400:173–177. [PubMed: 10408445]
3. Nicoll JA, Wilkinson D, Holmes C, Steart P, Markham H, Weller RO. Neuropathology of human Alzheimer disease after immunization with amyloid-beta peptide: a case report. Nat Med. 2003; 9:448–452. [PubMed: 12640446]
4. Orgogozo JM, Gilman S, Dartigues JF, Laurent B, Puel M, Kirby LC, Jouanny P, Dubois B, Eisner L, Flitman S, Michel BF, Boada M, Frank A, Hock C. Subacute meningoencephalitis in a subset of patients with AD after Abeta42 immunization. Neurology. 2003; 61:46–54. [PubMed: 12847155]
5. Weiner HL, Selkoe DJ. Inflammation and therapeutic vaccination in CNS diseases. Nature. 2002; 420:879–884. [PubMed: 12490962]
6. Gilman S, Koller M, Black RS, Jenkins L, Griffith SG, Fox NC, Eisner L, Kirby L, Rovira MB, Forette F, Orgogozo JM. Clinical effects of Abeta immunization (AN1792) in patients with AD in an interrupted trial. Neurology. 2005; 64:1553–1562. [PubMed: 15883316]
7. Bard F, Cannon C, Barbour R, Burke RL, Games D, Grajeda H, Guido T, Hu K, Huang J, Johnson-Wood K, Khan K, Kholodenko D, Lee M, Lieberburg I, Motter R, Nguyen M, Soriano F, Vasquez N, Weiss K, Welch B, Seubert P, Schenk D, Yednock T. Peripherally administered antibodies against amyloid beta-peptide enter the central nervous system and reduce pathology in a mouse model of Alzheimer disease. Nat Med. 2000; 6:916–919. [PubMed: 10932230]
8. Bacskai BJ, Kajdasz ST, McLellan ME, Games D, Seubert P, Schenk D, Hyman BT. Non-Fc-mediated mechanisms are involved in clearance of amyloid-beta in vivo by immunotherapy. Journal of Neuroscience. 2002; 22:7873–7878. [PubMed: 12223540]
9. Das P, Howard V, Loosbrock N, Dickson D, Murphy MP, Golde TE. Amyloid-beta immunization effectively reduces amyloid deposition in FcRgamma−/− knock-out mice. Journal of Neuroscience. 2003; 23:8532–8538. [PubMed: 13679422]
10. Ferrer I, Boada RM, Sanchez Guerra ML, Rey MJ, Costa-Jussa F. Neuropathology and pathogenesis of encephalitis following amyloid-beta immunization in Alzheimer's disease. Brain Pathol. 2004; 14:11–20. [PubMed: 14997933]
11. Hock C, Konietzko U, Streffer JR, Tracy J, Signorell A, Muller-Tillmanns B, Lemke U, Henke K, Moritz E, Garcia E, Wollmer MA, Umbricht D, de Quervain DJ, Hofmann M, Maddalena A,

Papassotiropoulos A, Nitsch RM. Antibodies against beta-amyloid slow cognitive decline in Alzheimer's disease. Neuron. 2003; 38:547–554. [PubMed: 12765607]

12. Grundman M, Black R. Clinical trials of bapineuzumab, a beta-amyloid-targeted immunotherapy in patients with mild to moderate Alzheimer's disease. Alzheimer's and Dementia. 2008; 4:T166.
13. Fukuchi KI, Accavitti-Loper M, Kim HD, Tahara K, Cao Y, Lewis TL, Caughey RC, Kim H, Lalonde R. Amelioration of amyloid load by anti-A[beta] single-chain antibody in Alzheimer mouse model. Biochemical and Biophysical Research Communications. 2006; 344:79–86. [PubMed: 16630540]
14. Fukuchi KI, Tahara K, Kim HD, Maxwell JA, Lewis TL, Accavitti-Loper M, Kim H, Ponnazhagan S, Lalonde R. Anti-Aβ single chain antibody delivery *via* adeno-associated virus for treatment of Alzheimer's disease. Neurobiol Dis. 2006; 23:502–511. [PubMed: 16766200]
15. Grimm D, Kay MA, Kleinschmidt JA. Helper virus-free, optically controllable, and two-plasmid-based production of adeno-associated virus vectors of serotypes 1 to 6. Mol Ther. 2003; 7:839–850. [PubMed: 12788658]
16. Zolotukhin S, Potter M, Zolotukhin I, Sakai Y, Loiler S, Fraites TJ Jr, Chiodo VA, Phillipsberg T, Muzyczka N, Hauswirth WW, Flotte TR, Byrne BJ, Snyder RO. Production and purification of serotype 1, 2, and 5 recombinant adeno-associated viral vectors. Methods. 2002; 28:158–167. [PubMed: 12413414]
17. Jankowsky JL, Fadale DJ, Anderson J, Xu GM, Gonzales V, Jenkins NA, Copeland NG, Lee MK, Younkin LH, Wagner SL, Younkin SG, Borchelt DR. Mutant presenilins specifically elevate the levels of the 42 residue beta-amyloid peptide in vivo: evidence for augmentation of a 42-specific gamma secretase. Hum Mol Genet. 2004; 13:159–170. [PubMed: 14645205]
18. DeMattos RB, Bales KR, Parsadanian M, O'Dell MA, Foss EM, Paul SM, Holtzman DM. Plaque-associated disruption of CSF and plasma amyloid-beta (Abeta) equilibrium in a mouse model of Alzheimer's disease. Journal of Neurochemistry. 2002; 81:229–236. [PubMed: 12064470]
19. Jin JJ, Kim HD, Maxwell JA, Li L, Fukuchi KI. Toll-like receptor 4-dependent upregulation of cytokines in a transgenic mouse model of Alzheimer's disease. J Neuroinflammation. 2008; 5:23. [PubMed: 18510752]
20. Pfeifer M, Boncristiano S, Bondolfi L, Stalder A, Deller T, Staufenbiel M, Mathews PM, Jucker M. Cerebral hemorrhage after passive anti-Abeta immunotherapy. Science. 2002; 298:1379. [PubMed: 12434053]
21. Racke MM, Boone LI, Hepburn DL, Parsadainian M, Bryan MT, Ness DK, Piroozi KS, Jordan WH, Brown DD, Hoffman WP, Holtzman DM, Bales KR, Gitter BD, May PC, Paul SM, DeMattos RB. Exacerbation of cerebral amyloid angiopathy-associated microhemorrhage in amyloid precursor protein transgenic mice by immunotherapy is dependent on antibody recognition of deposited forms of amyloid beta. Journal of Neuroscience. 2005; 25:629–636. [PubMed: 15659599]
22. Wilcock DM, Rojiani A, Rosenthal A, Subbarao S, Freeman MJ, Gordon MN, Morgan D. Passive immunotherapy against Abeta in aged APP-transgenic mice reverses cognitive deficits and depletes parenchymal amyloid deposits in spite of increased vascular amyloid and microhemorrhage. J Neuroinflammation. 2004; 1:24. [PubMed: 15588287]
23. Passini MA, Watson DJ, Vite CH, Landsburg DJ, Feigenbaum AL, Wolfe JH. Intraventricular brain injection of adeno-associated virus type 1 (AAV1) in neonatal mice results in complementary patterns of neuronal transduction to AAV2 and total long-term correction of storage lesions in the brains of beta-glucuronidase-deficient mice. J Virol. 2003; 77:7034–7040. [PubMed: 12768022]
24. Levites Y, Jansen K, Smithson LA, Dakin R, Holloway VM, Das P, Golde TE. Intracranial adeno-associated virus-mediated delivery of anti-pan amyloid beta, amyloid beta40, and amyloid beta42 single-chain variable fragments attenuates plaque pathology in amyloid precursor protein mice. Journal of Neuroscience. 2006; 26:11923–11928. [PubMed: 17108166]
25. Chakrabarty P, Ceballos-Diaz C, Beccard A, Janus C, Dickson D, Golde TE, Das P. IFN-gamma promotes complement expression and attenuates amyloid plaque deposition in amyloid beta precursor protein transgenic mice. Journal of Immunology. 2010; 184:5333–5343.
26. Kornum BR, Stott SR, Mattsson B, Wisman L, Ettrup A, Hermening S, Knudsen GM, Kirik D. Adeno-associated viral vector serotypes 1 and 5 targeted to the neonatal rat and pig striatum

induce widespread transgene expression in the forebrain. Experimental Neurology. 2010; 222:70–85. [PubMed: 20025873]

27. Markakis EA, Vives KP, Bober J, Leichtle S, Leranth C, Beecham J, Elsworth JD, Roth RH, Samulski RJ, Redmond DE Jr. Comparative transduction efficiency of AAV vector serotypes 1–6 in the substantia nigra and striatum of the primate brain. Mol Ther. 2010; 18:588–593. [PubMed: 20010918]
28. Taymans JM, Vandenberghe LH, Haute CV, Thiry I, Deroose CM, Mortelmans L, Wilson JM, Debyser Z, Baekelandt V. Comparative analysis of adeno-associated viral vector serotypes 1, 2, 5, 7, and 8 in mouse brain. Hum Gene Ther. 2007; 18:195–206. [PubMed: 17343566]
29. Banks WA, Terrell B, Farr SA, Robinson SM, Nonaka N, Morley JE. Passage of amyloid beta protein antibody across the blood-brain barrier in a mouse model of Alzheimer's disease. Peptides. 2002; 23:2223–2226. [PubMed: 12535702]
30. Levites Y, Das P, Price RW, Rochette MJ, Kostura LA, McGowan EM, Murphy MP, Golde TE. Anti-Abeta42- and anti-Abeta40-specific mAbs attenuate amyloid deposition in an Alzheimer disease mouse model. Journal of Clinical Investigation. 2006; 116:193–201. [PubMed: 16341263]
31. Wang YJ, Pollard A, Zhong JH, Dong XY, Wu XB, Zhou HD, Zhou XF. Intramuscular delivery of a single chain antibody gene reduces brain Abeta burden in a mouse model of Alzheimer's disease. Neurobiology of Aging. 2009; 30:364–376. [PubMed: 17686552]
32. Sudol KL, Mastrangelo MA, Narrow WC, Frazer ME, Levites YR, Golde TE, Federoff HJ, Bowers WJ. Generating differentially targeted amyloid-beta specific intrabodies as a passive vaccination strategy for Alzheimer's disease. Mol Ther. 2009; 17:2031–2040. [PubMed: 19638957]
33. Ryan DA, Mastrangelo MA, Narrow WC, Sullivan MA, Federoff HJ, Bowers WJ. Abeta-directed single-chain antibody delivery via a serotype-1 AAV vector improves learning behavior and pathology in Alzheimer's disease mice. Mol Ther. 2010; 18:1471–1481. [PubMed: 20551911]
34. Howard DB, Powers K, Wang Y, Harvey BK. Tropism and toxicity of adeno-associated viral vector serotypes 1, 2, 5, 6, 7, 8, and 9 in rat neurons and glia in vitro. Virology. 2008; 372:24–34. [PubMed: 18035387]
35. Royo NC, Vandenberghe LH, Ma JY, Hauspurg A, Yu L, Maronski M, Johnston J, Dichter MA, Wilson JM, Watson DJ. Specific AAV serotypes stably transduce primary hippocampal and cortical cultures with high efficiency and low toxicity. Brain Research. 2008; 1190:15–22. [PubMed: 18054899]
36. Li SF, Wang RZ, Meng QH, Li GL, Hu GJ, Dou WC, Li ZJ, Zhang ZX. Intra-ventricular infusion of rAAV1-EGFP resulted in transduction in multiple regions of adult rat brain: a comparative study with rAAV2 and rAAV5 vectors. Brain Research. 2006; 1122:1–9. [PubMed: 17045577]
37. Blits B, Derks S, Twisk J, Ehlert E, Prins J, Verhaagen J. Adeno-associated viral vector (AAV)-mediated gene transfer in the red nucleus of the adult rat brain: comparative analysis of the transduction properties of seven AAV serotypes and lentiviral vectors. J Neurosci Methods. 2010; 185:257–263. [PubMed: 19850079]
38. Reimsnider S, Manfredsson FP, Muzyczka N, Mandel RJ. Time course of transgene expression after intrastriatal pseudotyped rAAV2/1, rAAV2/2, rAAV2/5, and rAAV2/8 transduction in the rat. Mol Ther. 2007; 15:1504–1511. [PubMed: 17565350]
39. Tahara K, Kim HD, Jin JJ, Maxwell JA, Li L, Fukuchi KI. Role of toll-like receptor signalling in A{beta} uptake and clearance. Brain. 2006; 129:3006–3019. [PubMed: 16984903]
40. Smith EE, Greenberg SM. Beta-amyloid, blood vessels, and brain function. Stroke. 2009; 40:2601–2606. [PubMed: 19443808]
41. Patton RL, Kalback WM, Esh CL, Kokjohn TA, Van Vickle GD, Luehrs DC, Kuo YM, Lopez J, Brune D, Ferrer I, Masliah E, Newel AJ, Beach TG, Castano EM, Roher AE. Amyloid-beta peptide remnants in AN-1792-immunized Alzheimer's disease patients: a biochemical analysis. Am J Pathol. 2006; 169:1048–1063. [PubMed: 16936277]
42. Wilcock DM, Munireddy SK, Rosenthal A, Ugen KE, Gordon MN, Morgan D. Microglial activation facilitates Abeta plaque removal following intracranial anti-Abeta antibody administration. Neurobiol Dis. 2004; 15:11–20. [PubMed: 14751766]

43. Nicoll JA, Barton E, Boche D, Neal JW, Ferrer I, Thompson P, Vlachouli C, Wilkinson D, Bayer A, Games D, Seubert P, Schenk D, Holmes C. Abeta species removal after abeta42 immunization. J Neuropathol Exp Neurol. 2006; 65:1040–1048. [PubMed: 17086100]
44. Nicoll JA, Hawkes C, Holmes C, Weller R, Perry H, Boche D, Teeling J, Carare R. Processes underlying the vascular pathophysiology associated with As immunization in Alzheimer's disease. Alzheimers Dement. 2010; 6:S143.
45. Whitlow M, Bell BA, Feng SL, Filpula D, Hardman KD, Hubert SL, Rollence ML, Wood JF, Schott ME, Milenic DE. An improved linker for single-chain Fv with reduced aggregation and enhanced proteolytic stability. Protein Eng. 1993; 6:989–995. [PubMed: 8309948]
46. Wilcock DM, Colton CA. Immunotherapy, vascular pathology, and microhemorrhages in transgenic mice. CNS Neurol Disord Drug Targets. 2009; 8:50–64. [PubMed: 19275636]
47. Herzig MC, Winkler DT, Burgermeister P, Pfeifer M, Kohler E, Schmidt SD, Danner S, Abramowski D, Sturchler-Pierrat C, Burki K, van Duinen SG, Maat-Schieman ML, Staufenbiel M, Mathews PM, Jucker M. Abeta is targeted to the vasculature in a mouse model of hereditary cerebral hemorrhage with amyloidosis. Nat Neurosci. 2004; 7:954–960. [PubMed: 15311281]
48. Fryer JD, Simmons K, Parsadanian M, Bales KR, Paul SM, Sullivan PM, Holtzman DM. Human apolipoprotein E4 alters the amyloid-beta 40:42 ratio and promotes the formation of cerebral amyloid angiopathy in an amyloid precursor protein transgenic model. Journal of Neuroscience. 2005; 25:2803–2810. [PubMed: 15772340]
49. Taguchi H, Planque S, Nishiyama Y, Szabo P, Weksler ME, Friedland RP, Paul S. Catalytic antibodies to amyloid beta peptide in defense against Alzheimer disease. Autoimmun Rev. 2008; 7:391–397. [PubMed: 18486927]

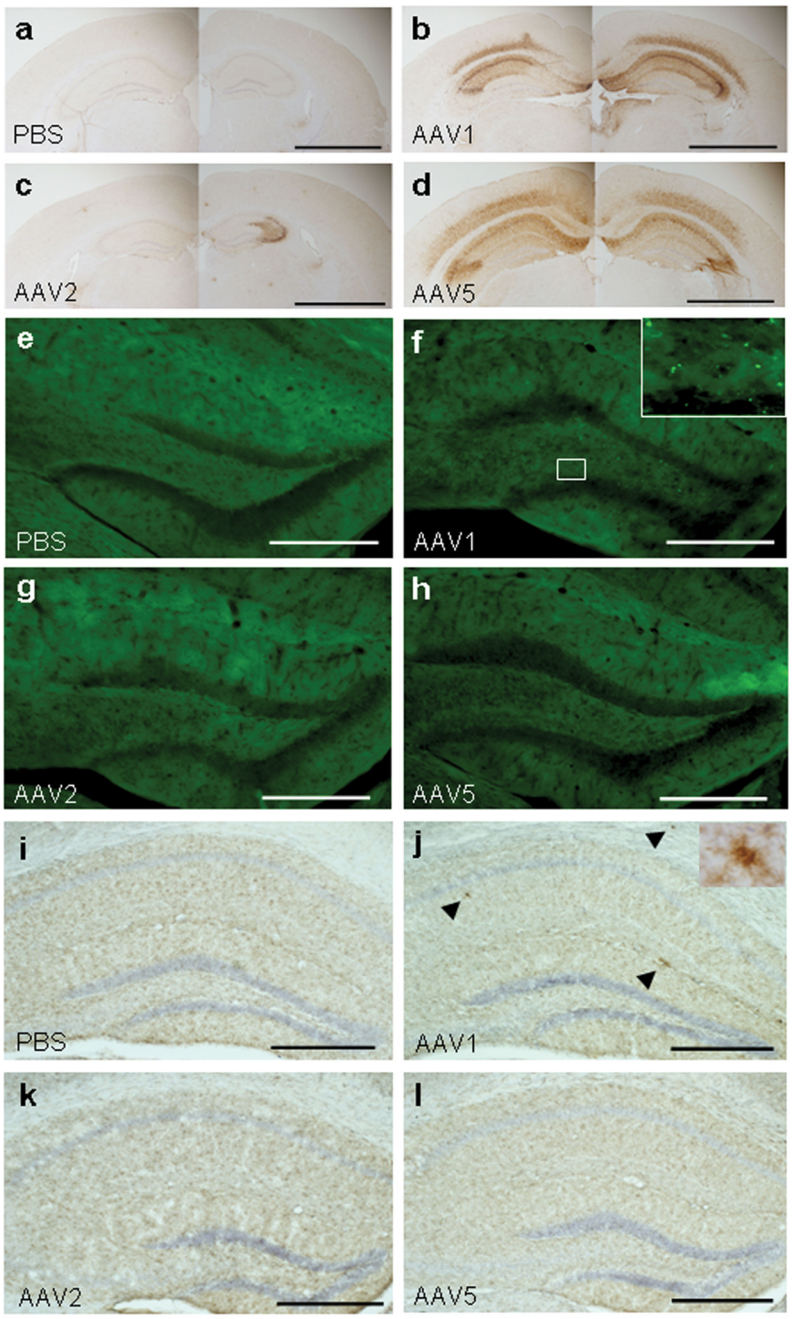

Figure 1. Optimization of scFv59 expression in the brain via rAAV serotype 1, 2, and 5 and their possible cytotoxicity in mice

Three serotypes of rAAV (1, 2, and 5) encoding scFv59 were injected into the right lateral ventricle of C57BL/6 mice and, 3 months after injection, scFv59 expressed in the brain was visualized by immunohistochemistry using anti-FLAG M2 antibody (scFv59 contains the FLAG sequence as a marker). (**a**) PBS-injected mice were used as negative controls. No staining is observed in PBS-injected mice. (**b**) Widespread, symmetrical expression of scFv59 is seen in both sides of the neocortex and the hippocampus in mice injected with rAAV1-CAscFv59. (**c**) Expression of scFv59 is limited mostly to a small part of the right hippocampus in mice subjected to rAAV2-CAscFv59 injection. (**d**) Widespread,

symmetrical expression of scFv59 in mice injected with rAAV5-CAscFv59, which resembles the expression pattern by rAAV1-CAscFv59. Levels of scFv59 expression in rAAV1-CAscFv59-injected mice are comparable to those in rAAV5-CAscFv59-injected mice. To assess cytotoxicity and inflammation potentially associated with AAV-mediated brain expression of scFv59, brain sections were subjected to TUNEL assay (**e**–**h**) and immunohistochemistry (**i**–**l**), respectively, using anti-CD11b antibody for activated microglia. Apoptotic cells identified by TUNEL are seen in the brain injected with rAAV1-CAscFv59 (**f**) but not in the brains injected with PBS (**e**), rAAV2-CAscFv59 (**g**), and rAAV5-CAscFv59 (**h**). The inset in (**f**) is a higher magnification of the boxed area. Scattered CD11b-positive cells are seen in the hippocampus of mice injected with rAAV1-CAscFv59 (**j**) but not in mice injected with PBS (**i**), rAAV2-CAscFv59 (**k**), and rAAV5-CAscFv59 (**l**). The inset in (**j**) is a higher magnification of one of CD11b-positive microglia indicated by arrow heads. Scale bars 2.0 mm (**a**–**d**) and 500 μm (**e**–**l**).

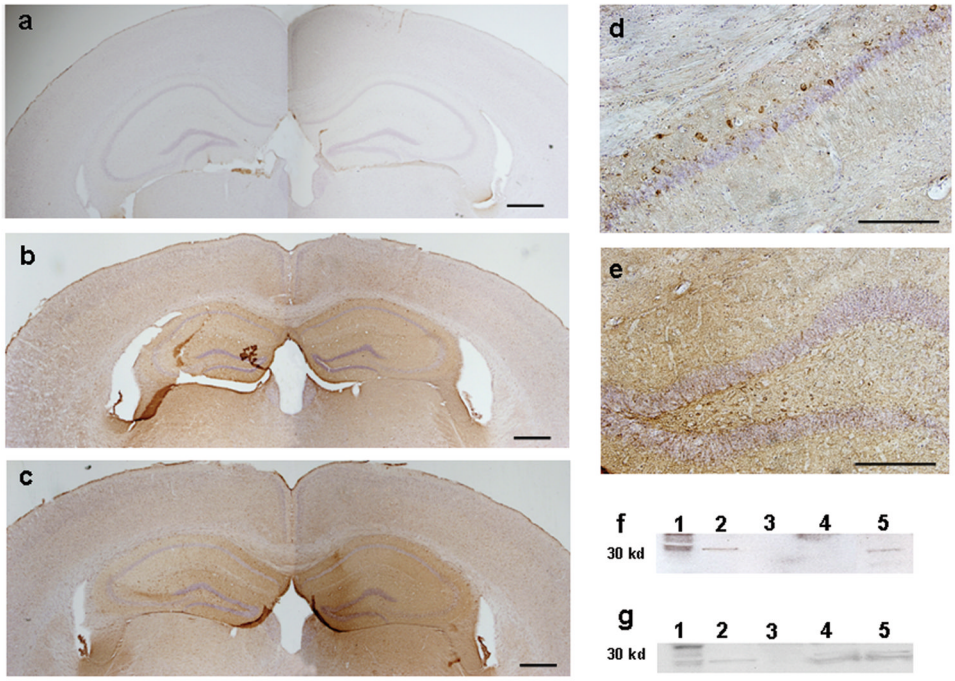

Figure 2. High expression levels of scFvs in the hippocampus and CSF in TgAPPswe/PS1dE9 mice five months after unilateral ventricular injection of rAAV5-scFvs a–e

Brain sections were prepared from TgAPPswe/PS1dE9 mice 5 months after rAAV5-scFv or PBS injection and subjected to immunohistochemical detection of scFvs using anti-FLAG M2 antibody (both scFv59 and scFv-Gag have the FLAG sequence as a marker). (**a**) PBS-injected brain showing no staining. (**b**) rAAV5-scFv-Gag-injected brain showing widespread, high expression of scFv-Gag in the hippocampus of both hemispheres and somewhat less expression in the neocortex. (**c**) rAAV5-scFv59-injected brain showing widespread, high expression of scFv-59 in the hippocampus of both hemispheres and somewhat less expression in the neocortex. (**d**) Cytoplasmic accumulation of scFv59 in CA1 hippocampal area in a mouse subjected to rAAV5-scFv59 injection. (**e**) The dentate gyrus showing a strong neuropil staining in a mouse subjected to rAAV5-scFv59 injection. Scale bars 400 μm (**a–c**) and 200 μm (**d** and **e**). (**f** and **g**) Five months after rAAV5-CAscFv59 injection, CSF (**f**) and hippocampal homogenates (**g**) were prepared and subjected to 10–20% SDS PAGE followed by western blotting using anti-FLAG M2 antibody. (**f**) scFv59 is identified as an approximately 30 kDa fragment in the CSF isolated from mice subjected to rAAV5-CAscFv59 injection. Lane 1: Molecular size markers; lane 2: Ten ng of purified scFv59 as a positive control; lane 3 Blank; lane 4: Ten μl of CSF from a PBS-injected mouse; and lane 5: Ten μl of CSF from a rAAV5-CAscFv59-injected mouse. (**g**) scFv59 is seen as 30–35 kDa fragments in the hippocampus of mice subjected to rAAV5-CAscFv59 injection. Lane 1: Molecular size markers; lane 2: Ten ng of purified scFv59 as a positive control; lane 3: Hippocampal homogenate from a PBS-injected mouse; and lane 4 and 5: Hippocampal homogenates from rAAV5-CAscFv59-injected mice.

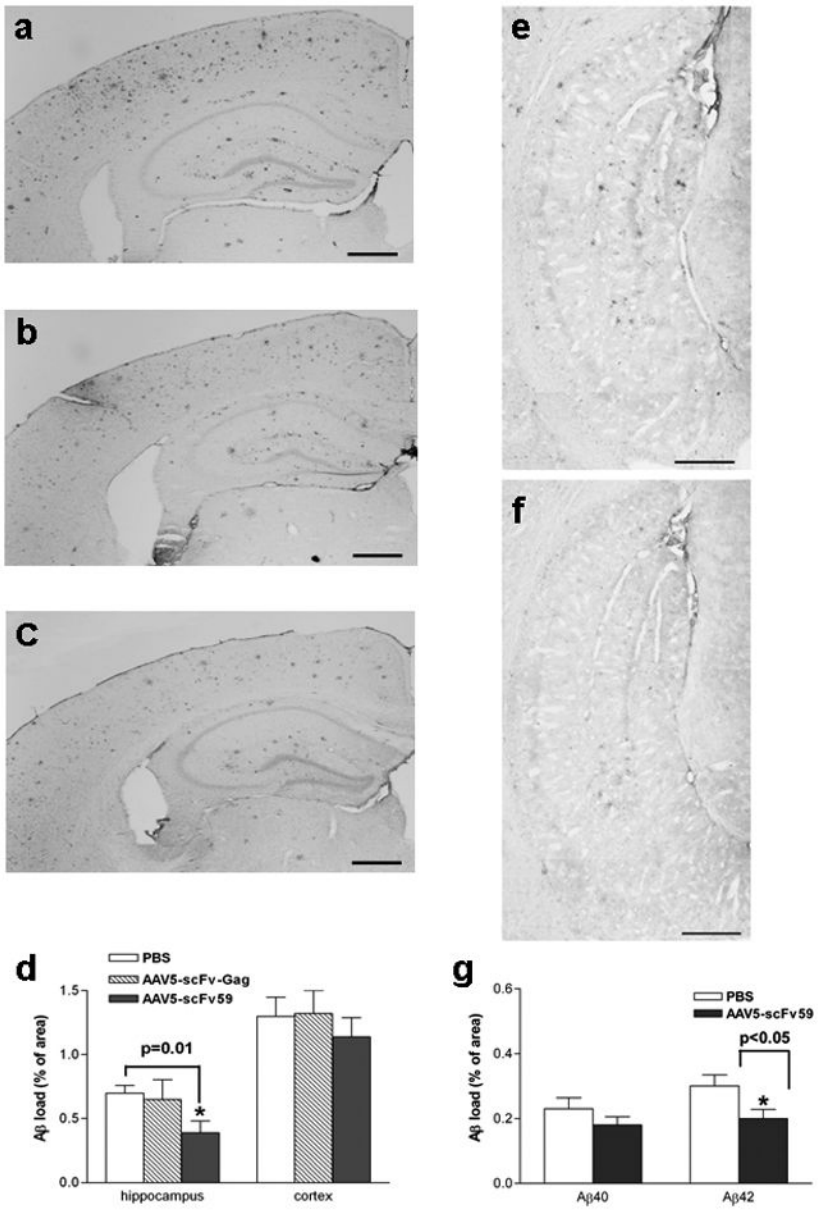

Figure 3. rAAV5-mediated scFv59 expression reduces immunoreactive Aβ deposits in the hippocampus but not in the neocortex

(**a, b, c, e** and **f**) Five months after rAAV5-CAscFv59, rAAV5-CAscFv-Gag, or PBS injection, mice were terminated and Aβ deposits in the brain were visualized by immunohistochemistry and quantified by morphometric analysis. Diffuse and fibrillar Aβ deposits visualized by 6E10 (**a–c**) and $A\beta_{42}$ C-terminal specific (**e** and **f**) antibody in the cerebral cortex (**a–c**) and hippocampus (**e** and **f**) from mice injected with PBS (**a** and **e**), rAAV5-CAscFv-Gag (**b**), and rAAV5-CAscFv59 (**c** and **f**). (**d** and **g**) The percentages of immunoreactive area for Aβ and $A\beta_{42}$, respectively, are shown as bar graphs. The values shown are the mean ± S.E.M. Scale bars 400 μm (**a–c**) and 200 μm (**e** and **f**).

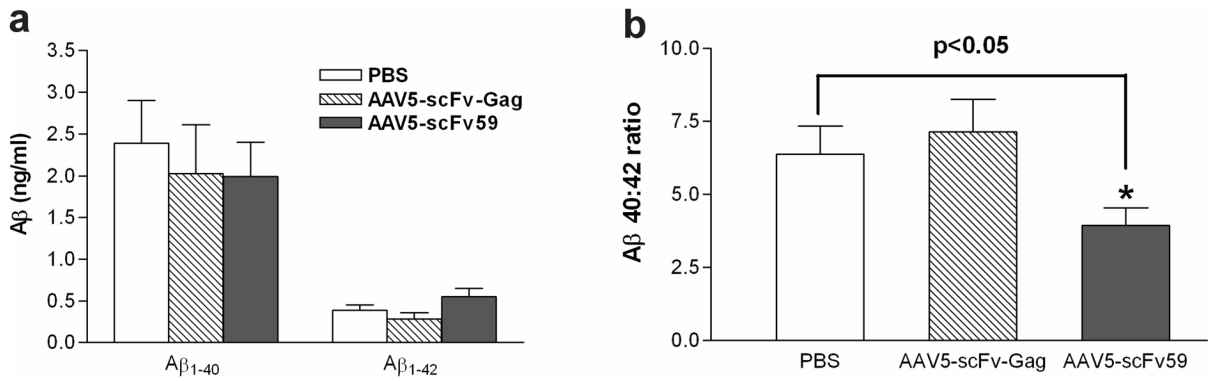

Figure 4. rAAV5-mediated scFv59 expression alters the $A\beta_{40}$:$A\beta_{42}$ ratio in CSF

Levels of $A\beta_{40}$ and $A\beta_{42}$ in the CSF were determined in mice 5 months after rAAV5-CAscFv59, rAAV5-CAscFv-Gag, or PBS injection. (**a**) Levels of $A\beta_{40}$ and $A\beta_{42}$ are shown as the means ± S.E.M. ng/ml. $A\beta_{42}$ levels in rAAV5-CAscFv59-injected mice increased by approximately 40% compared with PBS-injected mice but this did not reach statistical significance ($P = 0.1$). (**b**) The $A\beta_{40}$:$A\beta_{42}$ ratio in rAAV5-CAscFv59-injected mice is lower than that in rAAV5-CAscFv-Gag-injected and PBS-injected mice ($P < 0.05$). The values shown are the mean ±S.E.M.

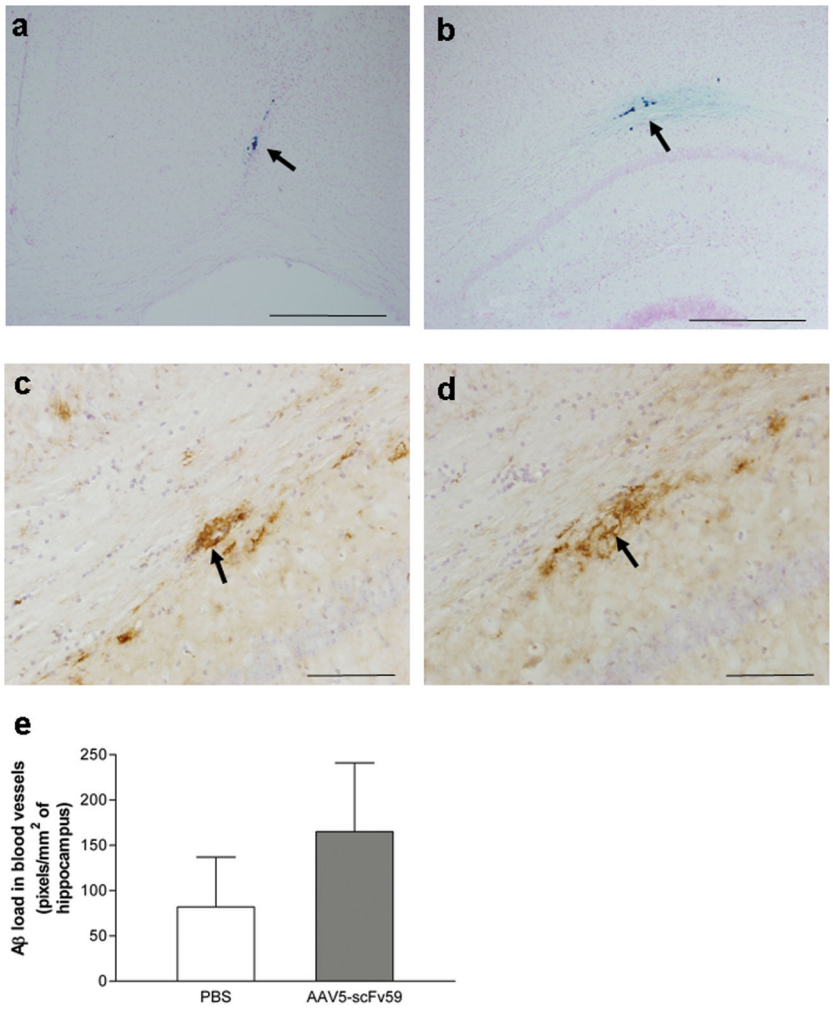

Figure 5. rAAV5-mediated scFv59 expression may cause cerebral hemorrhages

(**a** and **b**) Five months after rAAV5-CAscFv59, rAAV5-CAscFv-Gag, or PBS injection, mice were terminated and possible cerebral hemorrhages were detected by Prussian blue staining. (**a**) Blue spots indicating hemorrhage are scattered along with the needle track in the cortex 5 months after rAAV-CAscFv59 injection. (**b**) Hemorrhage is identified as blue spots in the corpus callosum in a TgAPPswe/PS1dE9 mouse subjected to rAAV5-CAscFv59 injection. (**c** and **d**) Aβ deposits focally increase in blood vessels in the corpus callosum where hemorrhage is found in the same mouse shown in **b**. (**e**) Quantitative analysis of vascular amyloid. The total pixels of Aβ-positive blood vessels per mm^2 in the hippocampus are shown as bar graphs. Data were expressed as mean ± S.E.M. Scale bars 500 μm (**a** and **b)** and 50 μm(**c** and **d)**.

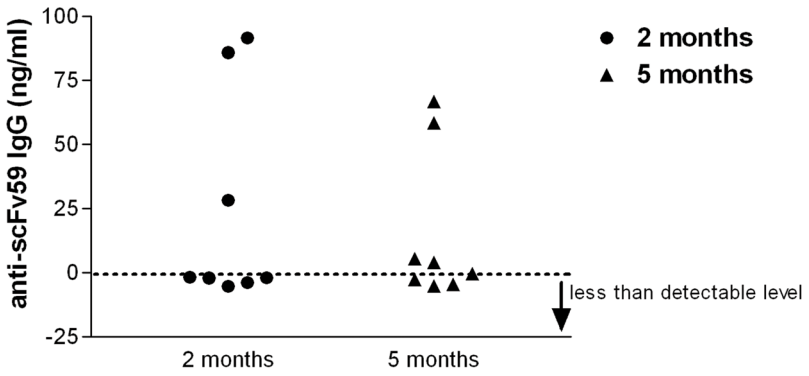

Figure 6. Induction of anti-scFv59 antibody by rAAV5-CAscFv59 injection is negligible

Two and five months after intraventricular injection of rAAV5-CAscFv59, sera were collected and anti-scFv59 IgG titers were determined by ELISA. Each anti-scFv59 titer from each TgAPPswe/PS1dE9 mouse subjected to rAAV5-CAscFv59 injection is shown.